Wind Stress Measurements from the Open Ocean Corrected for Airflow Distortion by the Ship

M. J. YELLAND, B. I. MOAT, P. K. TAYLOR, R. W. PASCAL, J. HUTCHINGS, AND V. C. CORNELL

James Rennell Division for Ocean Circulation, Southampton Oceanography Centre, Southampton, United Kingdom

(Manuscript received 27 March 1997, in final form 8 October 1997)

ABSTRACT

A large dataset of wind stress estimates, covering a wide range of wind speed and stability conditions, was obtained during three cruises of the RRS *Discovery* in the Southern Ocean. These data were used by Yelland and Taylor to determine the relationship between 10-m height, neutral stability values for the drag coefficient, and the wind speed, and to devise a new formulation for the nondimensional dissipation function under diabatic conditions. These results have been reevaluated allowing for the airflow distortion caused by the ship. The acceleration and vertical displacement of the flow have been modeled in three dimensions using computational fluid dynamics (CFD). The CFD modeling was tested, first by comparison with wind tunnel measurements on models of two Canadian research ships and second, by analysis of data from four anemometers on the foremast of the RRS *Charles Darwin.* Originally, the four anemometers gave drag coefficient values that differed by up to 20% from one to another and were all unexpectedly high. The CFD results showed that the airflow had been decelerated by 4%–14% and displaced vertically by about 1 m. These effects caused the original drag coefficient results to be overestimated by up to 60%. After correcting for flow distortion effects, the results from the different anemometers became consistent, which gave confidence in the quantitative CFD-derived corrections.

The CFD modeling showed that the anemometer position on the RRS *Discovery* was much less affected by airflow distortion. For a given wind speed the CFD corrections reduced the drag coefficient by about 6%. The resulting mean drag coefficient to wind speed relationship confirmed that suggested by Smith from a more limited set of open ocean data.

The effects of flow distortion are sensitive to changes in the relative wind direction. It is shown that much of the scatter in drag coefficient estimates may be due to variations in airflow distortion rather than to the effect of changing sea states. The *Discovery* wind stress data is examined for evidence of a sea-state dependence: none is found. It is concluded that a wave-age-dependent wind stress formulation is not applicable to open ocean conditions.

1. Introduction

Yelland and Taylor (1996, hereafter YT96) presented inertial dissipation wind stress measurements from the Southern Ocean, obtained from the Royal Research Ship *Discovery*. The exceptionally large dataset obtained (2464 ten-minute wind stress samples), and the wide range of conditions encountered, allowed them to develop a new formulation for the nondimensional dissipation function under diabatic conditions and to reevaluate the relationship between the 10-m neutral values for the drag coefficient C_{D10n}, and the wind speed U_{10n}. For $6 \leq U_{10n} \leq 26$ m s^{-1}, their predicted C_{D10n} values were about 5%–10% higher than the results of Smith (1980), Large and Pond (1981, 1982), or Anderson (1993). YT96 suggested that (following Smith et al. 1992) it was possible that the eddy correlation results of Smith (1980) might be low by a few percent and that the inertial dissipation results of Large and Pond and of Anderson might also have been low on average due to the inclusion of non-neutral data in the calculation of the mean relationship together with the assumption of zero imbalance in the kinetic energy budget. However, YT96 also offered an alternative explanation: that their own results might have been biased high due to the airflow distortion around the ship. They noted that preliminary results from computational fluid dynamics (CFD) modeling of the airflow around *Discovery* had shown that, even though the error induced in the mean wind speed was small, the lifting of the air flow over the bows of a ship was significant. Correcting for this effect would reduce the measured drag coefficient and bring the *Discovery* results closer to those of Smith (1980).

Since the publication of YT96, our further CFD modeling of the airflow around the *Discovery* and other ships has emphasized the vital importance of allowing for these effects when determining either the true wind

Corresponding author address: Dr. Margaret J. Yelland, James Rennell Centre for Ocean Circulation, Southampton Oceanography Centre, Room 254/26, Empress Dock, Southampton SO14 3ZH, United Kingdom.
E-mail: M.Yelland@soc.soton.ac.uk

or the wind stress (section 2). Although thorough validation of the CFD package will require an extensive program of shipboard measurements, we believe that the results to date are significant and have important consequences for all wind stress studies made from ships or other sizeable platforms. Section 2 describes the preliminary validation of the CFD results both by comparison with wind tunnel measurements and by showing that the CFD-derived corrections are able to reconcile previously anomalous data. The effects of flow distortion on the *Discovery* data are described in section 3. The CFD corrections modify the conclusions of YT96: the corrected *Discovery* data confirm the mean C_{D10n} to U_{10n} relationship suggested by Smith (1980).

The effect of the sea state on the wind stress has long been a subject for both experimental and theoretical study. From dimensional arguments, Charnock (1955) suggested that the roughness length z_0 and the friction velocity u_* could be related via a dimensionless ''constant'' α. Smith (1988) showed that a value of 0.011 for the constant was a good fit to the open ocean data of Smith (1980). However, other researchers have found different values for the constant depending on the measurement location. For example, for shallow water or coastal sites a constant of 0.018 has been suggested (Wu 1980), and measurements made over lakes have suggested higher values still (Geernaert 1990; Nordeng 1991). Donelan et al. (1993) summarized the many attempts to relate the different estimates of the Charnock constant to some measurable property of the sea state, often via a ''wave age'' parameter. This is usually defined as C_p/u_* or C_p/U_{10n} where C_p is the phase speed of the dominant wave at the peak of the wave spectrum. In summary, the majority of researchers suggest that the roughness length, and hence the wind stress, increases with decreasing wave age; that is, that for a given wind speed the drag coefficient will be larger in the presence of ''young'' or underdeveloped waves. Data from the HEXOS experiment, carried out from a platform in 18 m of water in the North Sea, resulted in a wave-age-dependent stress formulation (Smith et al. 1992) similar to that found by Donelan (1990) in an experiment on Lake Ontario. For shallow water, young wave environments these relationships predict an increase in the drag coefficient of up to 100% compared to long-fetch, deep water conditions (Kent et al., 1997, manuscript submitted to *J. Atmos. Oceanic Technol.*). The *Discovery* Southern Ocean data are examined for evidence to support such relationships for open ocean conditions (section 4). No evidence is found. The effects of flow distortion on the data are shown to depend strongly on the attitude of the ship to the wind direction. It is suggested that such effects may well explain the apparent variations of wind stress reported by previous authors, which have been ascribed to the effects of varying sea state.

2. Flow distortion and the use of CFD

a. Sensitivity of the C_{D10n} determination to airflow distortion

Determining C_{D10n} involves measurement of both the wind speed and the friction velocity u_* since, by definition

$$C_{D10n} = \left(\frac{u_*}{U_{10n}}\right)^2. \tag{1}$$

To determine u_* YT96 used, and describe in detail, the inertial dissipation method, which can be written

$$u_*^2 = \frac{f^{5/3}S_u(f)}{K}\left[\frac{2\pi}{U_{\rm rel}}\frac{kz}{(\phi_\varepsilon)}\right]^{2/3}, \tag{2}$$

where $S_u(f)$ is the spectral density of the wind speed measured at frequency f and height z, $U_{\rm rel}$ is the relative wind speed at the anemometer site, and k and K are the von Kármán and Kolmogorov constants, respectively. This study uses the form of the nondimensional dissipation function ϕ_ε given in YT96, which included an empirically derived estimate of the imbalance between production and dissipation of turbulent kinetic energy. Since the magnitude of likely errors in inertial dissipation estimates was considered in detail by Yelland et al. (1994, hereafter Y94), we shall here only discuss those errors caused by airflow distortion. In Eq. (2) the main variables to be determined by measurement are $S_u(f)$, $U_{\rm rel}$, and z. There is evidence that for the eddy sizes within the inertial subrange (order 1 m or less), the value of $S_u(f)$ is not significantly changed by the flow distortion. For example, comparison of data from instruments mounted on a well-exposed boom and a less well exposed mast demonstrated that the inertial dissipation method was much less affected by airflow distortion compared to the eddy correlation method (Edson et al. 1991). A similar conclusion was reached by Oost et al. (1994). With regard to $U_{\rm rel}$ the correct value to be used in Eq. (2) is that which is actually measured by the anemometer since that is the speed at which the turbulence is advected past the sensor. Acceleration of the flow due to flow distortion will be included in that measurement and will not cause an error in determining u_*. Thus, it is mainly through the estimation of the correct value for z that flow distortion might produce errors in the wind stress or u_*.

It is normally assumed that the measured value for $S_u(f)$ corresponds to turbulence at the height z of the anemometer. However, within the timescale that the turbulence can be considered frozen (of order seconds), the airflow may have changed height significantly [section 2d(2)]. Where the airflow has been raised due to the presence of the ship, the greater rate of turbulent intensity existing nearer the sea surface would be measured and associated with the instrument height. The value of u_* would therefore be overestimated. While Tillman et al. (1994) allowed for this effect in analyzing spectra from the Martian atmosphere, it has otherwise been ignored in studies of ocean surface wind stress.

Potentially the most serious flow-distortion-induced error occurs in determining C_{D10n} from Eq. (1), since it is necessary to know the true wind velocity. This is normally determined from the measured relative wind $U_{\rm rel}$ and the ship's velocity. Any flow-distortion-induced error in $U_{\rm rel}$ will cause an error in the calculated C_{D10n} value, regardless of the method (eddy correlation or inertial dissipation) used to obtain the friction velocity. If the aim is to determine the relationship between C_{D10n} and U_{10n}, then this error will have a double effect since if U_{10n} is biased high, C_{D10n} will be biased low (and vice versa).

The potential size of each of these errors is significant. A 3% underestimate of the true wind speed will be equivalent to an overestimate of C_{D10n} (for a given wind speed) varying from 7% to 8% for wind speeds in the range 1–25 m s^{-1}. A similar drag coefficient error would be caused by a 10% rise in the airflow height, that is, a vertical displacement of 1–2 m for typical anemometer heights of 10–20 m.

b. Previous estimates of wind speed errors

Previous authors have reported comparisons between mast and bow boom mounted anemometers (Ching 1976; Kidwell and Seguin 1978) and between ship measurements and meteorological buoys (Augstein et al. 1974; Godshall et al. 1976; Reynolds 1982; Weller et al. 1983). It is difficult to obtain consistent results from such comparisons. For example, the difficulty of obtaining reliable wind data from buoys was emphasized by Weller et al. (1990), and Queffeulou (1991) even suggests the need for ship-derived wind data to intercalibrate a buoy array. However, the comparisons do indicate that typical magnitudes for the wind speed errors for ship-mounted instruments are perhaps $\pm 5\%$ for winds within $\pm 45°$ of the bow, and possibly much larger for other relative wind directions.

Wind tunnel studies conducted on ship models provide estimates of wind speed errors at chosen anemometer sites for a wide range of relative wind directions. For example, for a research vessel, Romanov et al. (1983) found wind speed errors of -5% at the end of a bow boom, -3% on the foremast, and $+1\%$ on the mainmast when the wind was on the bow. With the wind on the beam the wind speed was overestimated; by over $+10\%$ for the foremast site and $+5\%$ on the mainmast. For two warships, Blanc (1986, 1987) found that the wind speed was overestimated, for bow winds, by about 10% at the mainmast anemometer positions. Wind tunnel studies for two Canadian research ships (Surry et al. 1989; Thiebaux 1990) will be used below in evaluating our own results. These studies also indicated an overestimation of the wind speed by about 5% for a mainmast anemometer site.

Increased wind speeds at mainmast anemometer sites have also been predicted by numerical modeling. Using a potential flow model, Kahma and Lepparanta (1981) predicted errors of about 15% for a small research vessel, the R/V *Aranda.* Dupuis (1994, personal communication) has used a CFD model to predict a wind speed increase of about 20% at the mainmast anemometer site on the research ship *Le Suroit.* However, both these studies were two-dimensional, implying an infinitely wide ship, and the errors might have been overestimated.

In summary, previous results from field experiments, wind tunnel studies, and numerical modeling all suggest typical wind speed errors of 5%–10%. This would imply possible errors in the value of C_{D10n}, for a given wind speed, of 12%–25% and possibly more.

c. Use of CFD to determine the airflow distortion

1) THE COMPUTATIONAL FLUID DYNAMICS PACKAGE

The numerical model used for the three-dimensional computation of the airflow was a finite volume, commercially available CFD package called ''Vectis'' (Ricardo 1994). A commercially available finite element preprocessor, ''Femgen'' (Femsys 1994), was used to form the surface geometry of the ship from a digitized set of ship's plans. This ship model was enclosed in a computational domain that simulated a large rectangular ''wind tunnel'' equivalent to 600 m long, 300 m wide, and 150 m high (typical ship dimensions are less than 100 m in length and 20 m in width).

A variable density computational mesh was generated inside the wind tunnel by the CFD package, allowing the models to have fine resolution (minimum cell dimension $\approx$ 20 cm) in areas of interest while using a much coarser resolution in regions well away from the ship. The simulations included around 200 000 computational cells and required about four weeks of processor time on a dedicated Silicon Graphics Indigo[2] R8000 machine with 288 Mb of memory before converging on a steady solution. This has limited the number of CFD evaluations that have been performed, and the present results only apply to a restricted range of relative wind speeds and directions, as will be discussed below.

During each simulation, the vertical profile of the wind speed 100 m abeam of the ship, halfway along the tunnel, was compared to the inlet wind profile to ensure that the ship was not causing significant blockage of the air flow through the tunnel. Streamlines from the tunnel inlet were used to estimate the original height z_f of the flow reaching the anemometer site. This was used as the value for z in Eq. (2). Velocity data were extracted for the anemometer sites and compared to the velocity at height z_f in a region of free stream flow, well away from the ship. Hence, for each anemometer site, the

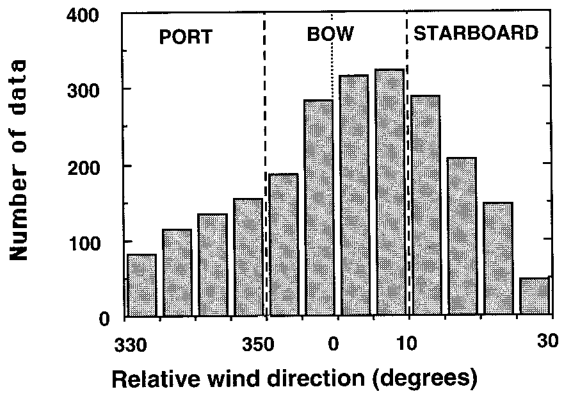

FIG. 1a. Distribution of relative wind directions for the data from RRS *Discovery* (corresponding to relative wind speeds over 6 m s^{-1}) as used by Yelland and Taylor (1996) and the subset of data (wind within $\pm10°$ of the bow) used in this study.

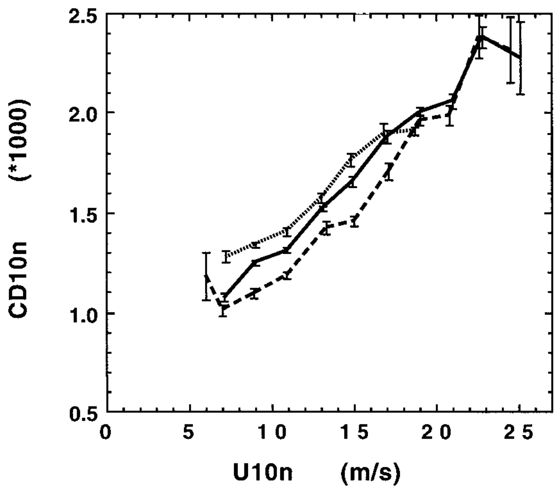

FIG. 1b. Mean drag coefficient values (averaged as a function of 10-m neutral wind speed) for the RRS *Discovery* data used by Yelland and Taylor (1996). The data have been separated according to relative wind direction: the solid line indicates winds over the bow ($\pm10°$); the dashed line, winds from the port bow (330°–350°); and the dotted line, winds from starboard (10°–30°). Error bars indicate standard deviation of the mean.

mean wind speed error ΔU and the vertical displacement of the flow Δz could be found.

2) RANGE OF RELATIVE WIND DIRECTION

Most published C_{D10n} data has been obtained from research ships while hove to, that is, with the ship stationary or moving very slowly through the water and with the relative wind blowing from ahead of the ship. For that reason, all of the ships were modeled in the CFD simulations with the wind blowing directly over the bow.

Observations suggest that changes in the relative wind direction can significantly alter the results. YT96 used all data when the wind was within 30 degrees of the bow (Fig. 1a). Figure 1b shows the C_{D10n} results after the data have been separated into three relative wind direction classes: ''port'' and ''starboard'' for relative wind directions of more than 10 (and less than 30) degrees to port or starboard of the bow, and ''bow'' for relative wind directions within 10 degrees of the bow. For a given U_{10N} it can be seen that over most of the wind speed range the drag coefficients obtained with the wind on the starboard bow are overestimated by about 5% compared to the bow-on values, and those from the port bow are underestimated by about 10%. This asymmetry is to be expected since the anemometer was mounted on the starboard edge of the platform, as far as possible from the foremast extension in the center of the platform. The effect of relative wind direction on the mean C_{D10n} to U_{10n} relationship derived from the whole dataset was small, since the errors in the port bow data were fortuitously cancelled out by those from the starboard bow data. However, only data obtained when the wind was within $\pm10°$ of the bow will be considered further in this paper.

3) RANGE OF WIND SPEED

The YT96 results were similar to other studies in showing a minimum in the drag coefficient relationship at about 6 m s^{-1}. At lower wind speeds, observed C_{D10n} values show large scatter and, as free convection is approached, u_* is no longer an appropriate scale for the boundary layer parameters. It is also likely that, at some critical wind speed below 6 m s^{-1}, the pattern of flow around the ship may change (for example see Kidwell and Seguin 1978). This paper will only consider data for wind speeds of 6 m s^{-1} and greater. For the open ocean this represents almost all the data. For example, YT96 obtained only 166 wind stress values at winds below 6 m s^{-1} compared to 2298 at higher wind speeds. Of the latter, 1111 data corresponded to our criterion of relative wind direction within $\pm10°$ of the bow.

d. Validation of the CFD results

1) COMPARISON WITH WIND TUNNEL STUDIES

In order to evaluate the accuracy of the ΔU estimates from the CFD model, the air flow over the Canadian research ships CSS *Hudson* and CSS *Dawson* were first simulated, since these ships had previously been tested in a boundary layer wind tunnel by Surry et al. (1989). Both ships carried an anemometer on the mainmast and an additional anemometer mounted in the bow.

To allow quantitative comparison with the wind tunnel results, the ships were modeled using a logarithmic wind profile with a wind speed of 13 m s^{-1} at a height of 10 m. Table 1 summarizes the mean wind speed errors, ΔU, as a percentage of the undisturbed wind speed, for the mainmast and bow anemometer sites. Both the CFD and wind tunnel results suggested accelerated flow of about 6%–7% at the mainmast anemometer and decelerated flow by up to 3% at the bow anemometer. The

TABLE 1. Vertical displacement of airflow and wind speed errors at anemometer sites from CFD model and wind tunnel tests. A negative wind speed error implies that the airflow has been decelerated and that the wind speed from the anemometer would be an underestimate.

	CFD model results				Wind tunnel results	
Ship	Mainmast Δz (m)	Bow Δz (m)	Mainmast ΔU (%)	Bow ΔU (%)	Mainmast ΔU (%)	Bow ΔU (%)
CSS *Dawson*	1.1	0.4	+5.5	−0.2	+7.0	−1.0
CSS *Hudson*	2.4	1.1	+6.0	−3.3	+6.0	−1.0

largest difference between the wind tunnel and CFD results was for the bow anemometer on *Hudson.* However, Fig. 2, which reproduces the wind speed errors from the tables in Thiebaux (1990), suggests that the wind tunnel results may have been in error by showing a spuriously large variation in ΔU with wind direction in the immediate vicinity of the bow. Apart from that one data point, the wind tunnel results confirm that the CFD wind speed corrections calculated for bow winds are applicable to data obtained for relative wind directions within $\pm 10°$ of the bow. Significantly different corrections would be required to correct data obtained for other relative wind directions.

The wind tunnel results did not include estimates for the change in height of the airflow. However, observations suggest that the CFD predictions are of the correct order. Thus, Dobson et al. (1994, 1995) show C_{D10n} observations from the *Hudson* that, in the mean, are about 10%–30% greater than the results of Anderson (1993), obtained on the *Dawson.* Taken in isolation, the CFD derived corrections for the wind speed would suggest that the *Hudson* C_{D10n} values should only be 5%–15% greater than those from the *Dawson.* Allowing for the change in height of the airflow increases the predicted overestimate for the *Hudson* to the range 8%–22%, closer to that observed. If it is assumed that the CFD-predicted ΔU values are correct (since they agree with the wind tunnel measurements), then the inference is that the CFD predicted Δz values are correct or slightly underestimated.

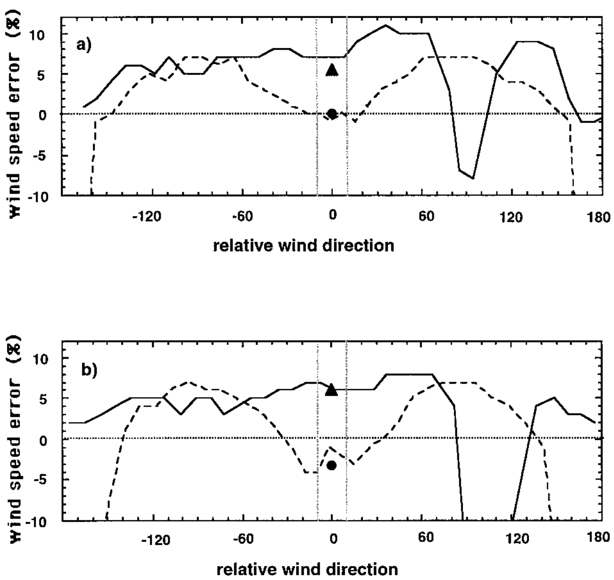

FIG. 2. Wind speed errors at the bow (dashed lines) and mainmast (solid lines) anemometer sites as measured in wind tunnel studies of (a) the *Dawson* and (b) the *Hudson* (Thiebaux 1990). The CFD model results are shown as a circle for the bow anemometer site and a triangle for the main mast site (see also Table 1). Relative wind directions within $\pm 10°$ of the bow are indicated by the vertical lines.

2) REMOVAL OF BIASES FROM SIMULTANEOUS WIND STRESS ESTIMATES

Yelland et al. reported data from four anemometers mounted on the foremast of the research ship *Charles Darwin* (Fig. 3). The foremast was situated well forward in the bow of the ship and appeared to be well exposed for winds from ahead. However, for a given U_{10n}, the calculated C_{D10n} values were significantly larger than those of YT96 and varied by 12%–20% from one anemometer to another. Because the observed friction velocity values agreed to better than 3%, Y94 concluded that the C_{D10n} differences were caused by errors in estimating the wind speed [see Eq. (1)]. Differences in the measured mean relative wind speed ranging up to 8% were ascribed to airflow distortion in the region of the anemometer sites. These data therefore provide a good test of the ability of the CFD package to predict, and provide corrections for, the effects of flow distortion.

Figure 4 shows results from the three-dimensional CFD modeling of the airflow around the *Charles Darwin.* Data on a vertical plane that intersects the Solent sonic anemometer position are shown. The ratio between the actual wind speed at any point and the freestream wind speed (i.e., the wind speed at that point undistorted by the presence of the ship) has been used to indicate the magnitude of the wind speed errors on the vertical plane. Ratios with a value greater than 1.0 indicate that the presence of the ship has accelerated the airflow. The length and shading of the arrows indicate the size of the wind speed ratio, and the direction of the arrow indicates the direction of the airflow. The results from each computational cell are shown by a separate arrow: the greater mesh densities around regions of interest are apparent.

The superstructure of the *Charles Darwin* forms an abrupt blockage relatively close to the foremast. The region of decelerated air in front of the superstructure

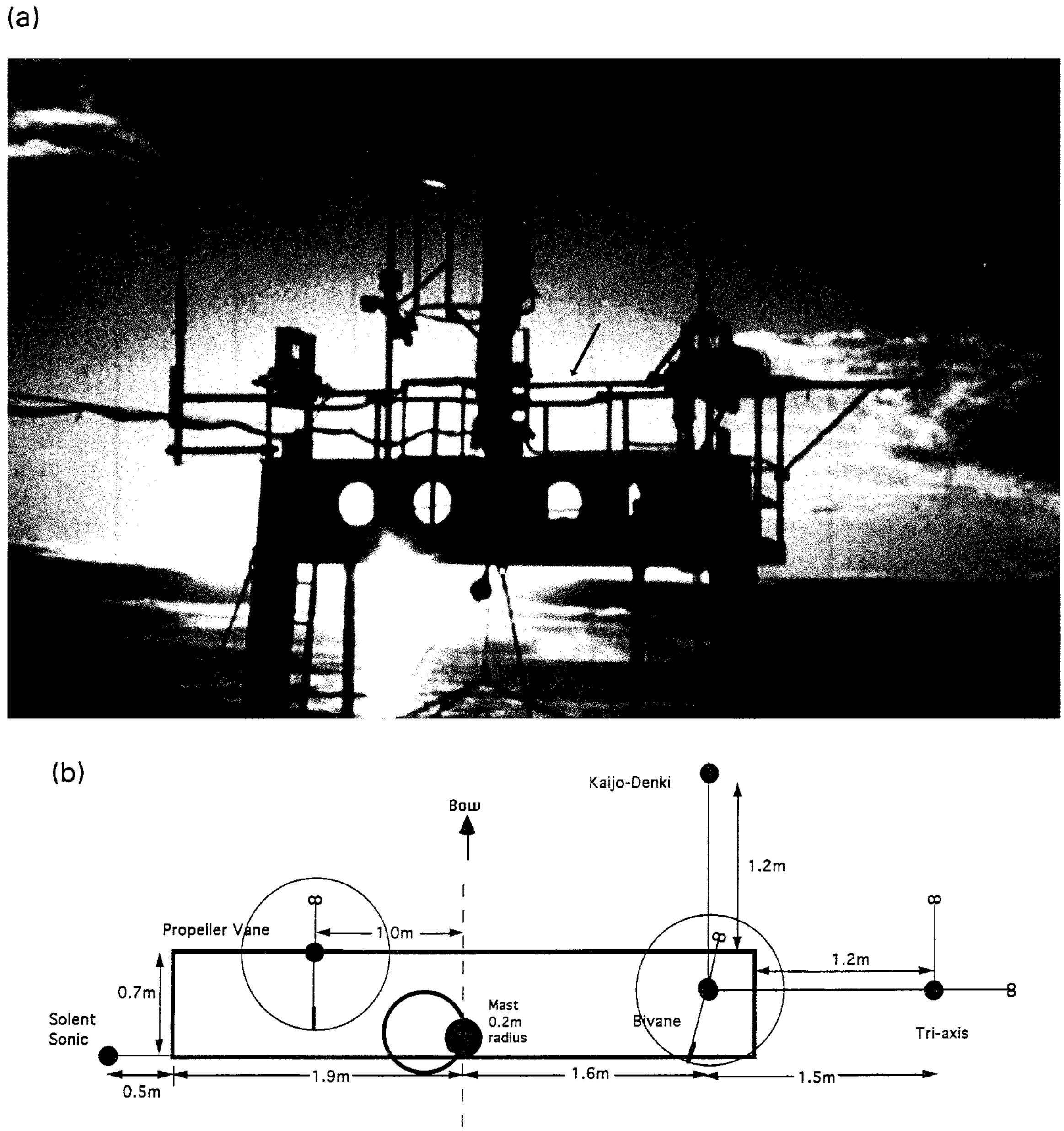

FIG. 3. (a) The foremast platform of the RRS *Charles Darwin* (photographed from the port bridge wing). From left to right the anemometers (and their heights) are a Solent sonic (15.1 m), a Young propeller–vane (15.6 m), a Young bivane (15.7 m), a Kaijo-Denki sonic (position forward of the platform indicated by the arrow, 14.3 m), and a Young tri-axis (not used). (b) Plan view of the platform (reproduced from Yelland et al. 1994).

extends forward to the foremast platform, causing large wind speed errors at the anemometer sites. The Solent sonic, propeller–vane, and bivane instruments, mounted above the foremast platform, were in a region where the wind speed had been decelerated by between 3% and 9% from the undisturbed value (Table 2). The Kaijo-Denki anemometer was situated in front of the foremast platform. This also presented a blockage to the flow of air and caused the measured wind speed at this anemometer site to be reduced by more than 13% from the undisturbed value. The airflow had been displaced vertically by 1 m at the site of the Kaijo-Denki and by 1.2 m at the other anemometer sites, which were mounted slightly higher and farther aft. The displacement began 40 m (or 2.9 s) upstream of the site, but half of the displacement took place within 8 m (0.6 s) of the anemometer. Since the correlation, or "memory," time of the turbulence has been estimated to be of the order of 5 s or more (Henjes 1996), this suggests that the turbulence will not have adjusted to the vertical displace-

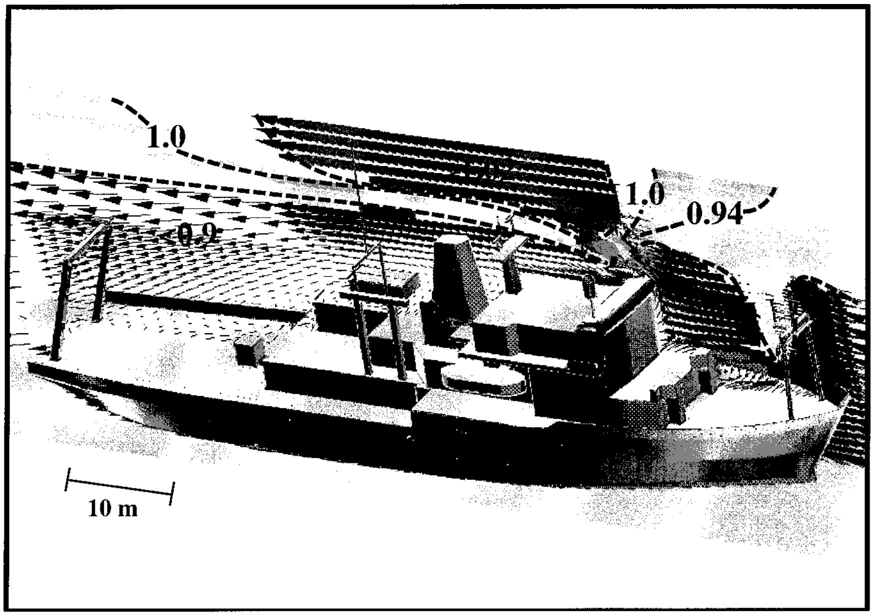

FIG. 4. CFD model results for flow over the RRS *Charles Darwin.* Only data on a vertical plane intersecting the Solent sonic anemometer site are shown. The results are expressed as the ratio between the actual wind speed at any point and the freestream wind speed (i.e., the wind speed at that point undistorted by the presence of the ship). This ratio governs the length and shading of the arrows, the direction of which indicates the direction of flow around the ship. Each arrow is associated with a single computational cell.

ment by the time the flow reaches the anemometer site (section 2a). The CFD prediction that the flow of air is displaced vertically by a similar amount at all the anemometer sites is consistent with the observation (Y94) that the friction velocities from the four instruments were in good agreement. However, it also suggests that all of the observed u_* values were biased by a similar extent.

The angle of the airflow to the horizontal at the anemometer sites was between 6° and 9° for the *Darwin* anemometers. These CFD results were in accord with the measured components of wind speed from the Solent sonic anemometer. Although it is difficult to know the precise vertical alignment of a shipborne instrument, the Solent sonic indicated a deviation of the wind flow from the horizontal of 7° when the wind was over the bow (Yelland et al. 1991), in good agreement with the CFD value of 6°. Similar information from the Kaijo-Denki anemometer was not available. Whereas the sonic anemometers measured all three components of wind speed, and the bivane anemometer oriented itself into the mean flow, the propeller–vane anemometer only measured the horizontal component of the mean wind and a correction is required. Assuming a cosine response, an increase of 1% was made to the wind speed from the propeller–vane anemometer to allow for the 9° angle of the flow predicted by the CFD simulation at that anemometer site.

In order to determine the effect of the CFD predicted errors on the wind stress values the *Darwin* cruise data were reanalyzed selecting only data samples collected for winds within ±10° of the bow. This amounted to approximately half of the 146 ten-minute samples used by Y94 (the remainder were all obtained with the relative wind farther to port, 340°–350°). The form of the dissipation function used followed that of YT96, rather than Y94: this further increased the calculated mean drag coefficients by about 10%, that is, the discrepancy with YT96 was increased still further. Although the data from the two sonic anemometers was the least scattered (see Y94), these instruments showed the largest systematic differences in measured wind speed, resulting in drag coefficients that differed by about 25% at the higher wind speeds. The average drag coefficients from the four anemometers differed by up to 20%. Based on this reanalysis, the mean drag coefficient relationship from the four anemometers used on the *Darwin* cruise was up to 40% larger than that reported by YT96 for the *Discovery* cruises (Fig. 5).

TABLE 2. Wind speed errors ΔU, vertical displacement of airflow Δz, and the angle of the flow to the horizontal ϕ, at the anemometer sites on RRS *Charles Darwin* as calculated from the CFD model.

Anemometer	Height (m)	ΔU (%)	Δz (m)	ϕ (°)
Solent sonic	15.1	−3.5	1.2	6
Propeller-vane	15.6	−9.0	1.2	9
Bivane	15.7	−6.0	1.2	8
Kaijo-Denki	14.3	−13.5	1.0	7

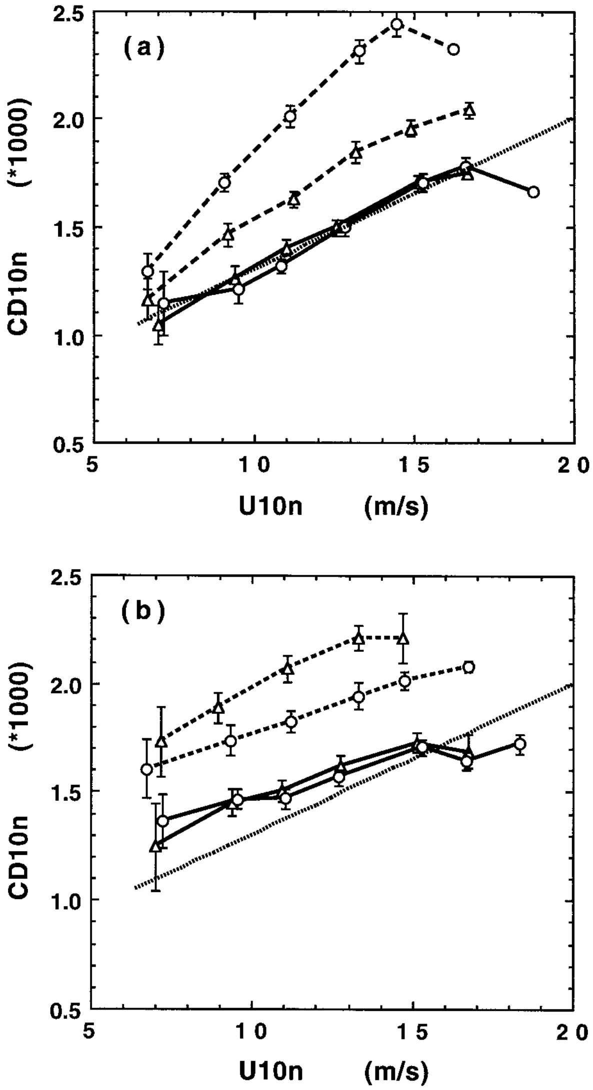

FIG. 5. (a) The drag coefficient to wind speed relationships from the two sonic anemometers on the foremast of the *Darwin* before (dashed lines) and after (solid lines) correcting the data for airflow distortion. Error bars indicate standard deviation of the mean. The dotted line is the YT96 relationship; △: Solent Sonic; and ○: Kaijo Denki. (b) As in (a) but for the two propeller anemometers, △: Young Propeller–vane and ○: Young bivane.

Applying the corrections for airflow distortion greatly reduced the calculated drag coefficients from all four anemometers. The C_{D10n} values obtained from the Solent sonic anemometer, located in the region of least flow distortion, were reduced by up to 15%, whereas those from the Kaijo-Denki were reduced by up to 45%, bringing the results from the two instruments into close agreement (Fig. 5a). The corrected sonic anemometer data were now similar to the YT96 relationship (shown for comparison): however, it must be remembered that application of the CFD corrections will also change the *Discovery* data (section 3a below). The C_{D10n} values estimated using the propeller anemometers were also

TABLE 3. Wind speed errors ΔU, vertical displacement of airflow Δz, and the angle of the flow to the horizontal ϕ, at the site of the Solent Sonic anemometer (height 18.5 m) on RRS *Discovery* for three different values of the 10-m wind speed.

U_{10} (m s^{-1})	ΔU (%)	Δz (m)	ϕ (°)
6	−0.3	1.2	2
14	−0.5	1.0	2
20.5	−0.8	0.7	2

significantly decreased (Fig. 5b). For the higher wind speeds, all four anemometers were brought into good agreement. At lower wind speeds, the drag coefficients from the two propeller anemometers were up to 20% larger than those from the sonic anemometers. This was probably due to the use of too large a response correction for the propeller instruments at the lower wind speeds (Y94).

Overall, the difference in the average drag coefficients from the four anemometers was reduced from a maximum of 20% for the uncorrected data to 5% or better for the corrected data. That the CFD-derived correction factors reconciled these previously disparate results from Y94 gives confidence that the CFD results are quantitatively correct as well as being qualitatively reasonable.

3. The mean open ocean drag coefficient relationship

a. *Airflow distortion over the RRS* Discovery

The data from the RRS *Discovery* cruises in the Southern Ocean used by YT96 cover a wide range of wind speed and stability conditions. Most of the data were obtained when the ship was hove to or steaming slowly into the wind. The shape of the vertical profile of the relative wind will have varied from logarithmic (for the ship stationary and a neutral stability surface layer flow) to a slab profile (for the ship under way in calm weather). However, there was not enough data obtained with the ship under way to determine observationally whether the measured drag coefficient was affected by this modification of the relative wind profile by the ship velocity.

To simulate these conditions, three separate CFD simulations were performed, with 10-m wind speeds equivalent to 6, 14, and 20.5 m s^{-1}. The shape of the CFD modeled wind profiles were such that the slowest wind speed run was equivalent to a stationary ship, whereas the other two model runs were equivalent to a ship under way at 3 m s^{-1} into true wind profiles with a U_{10n} of 11 and 17.5. The results are summarized in Table 3. In all cases, the airflow reaching the Solent sonic anemometer site had been raised by about 1 m and decelerated by less than 1%. Both of these effects act in the same sense, causing the value of C_{D10n} for a given wind speed to be overestimated by, in total, about 6%. A

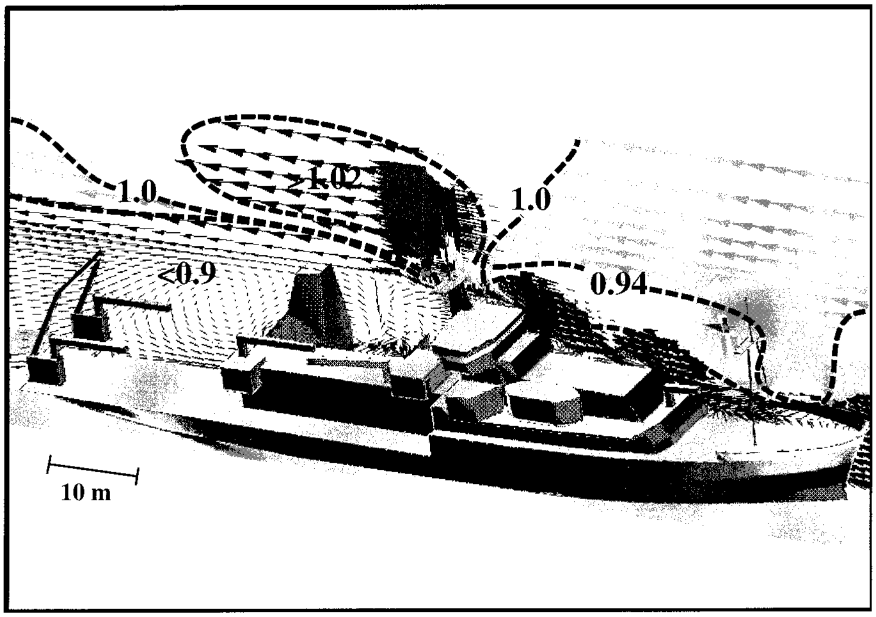

FIG. 6. As in Fig. 4 but for flow over the RRS *Discovery.* The image has been reversed (port to starboard) to expose more of the ship structure.

similar overestimate was obtained for each of the simulations. The changes in ΔU and Δz were such that the effect of the increased wind speed error at higher wind speeds was cancelled by the smaller height change. This was confirmed by using each pair of calculated ΔU and Δz values in turn to reanalyze the data from the *Discovery.* The calculated C_{D10n} to wind speed relationships were indistinguishable at all but the highest wind speeds, where the maximum difference in the mean drag coefficients was less than 2%. Thus, the combined effect of the changes in relative wind speed, and in the deviation of the profile from logarithmic, made no discernible difference to the calculated results.

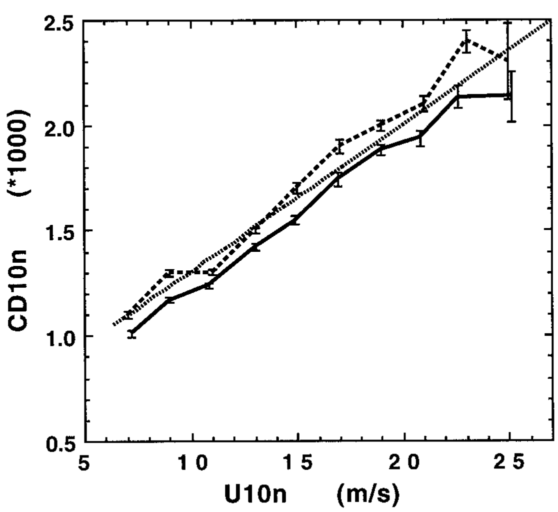

FIG. 7. The drag coefficient to wind speed relationships from the *Discovery* data within ±10° of the bow before (dashed lines) and after (solid lines) correcting the data for airflow distortion. Error bars indicate standard deviation of the mean. The dotted line is the YT96 relationship that was derived using data within ±30° of the bow.

For the remainder of this paper it will be assumed that the results from a CFD simulation using a 10-m wind speed of 14 m s^{-1} can be applied to all data obtained at wind speeds of 6 m s^{-1} or more. Based on that simulation, Fig. 6 shows wind speed errors, as a percentage of the undisturbed value, on a vertical fore–aft plane through the Solent sonic anemometer position on the *Discovery.* It can be seen that the superstructure of this ship is relatively streamlined and that the foremast platform is situated well above the region of decelerated flow that occurs in front of the accommodation block. Hence, the airflow corrections needed for the *Discovery* data (Table 3) are much smaller than those needed for the *Charles Darwin* (Table 2).

The effects of the corrections on the *Discovery* data are shown in Fig. 7. The CFD-corrected C_{D10n} values lie parallel to but about 0.1 ($\times 10^{-3}$) lower than the YT96 relationship. Comparison with the CFD-corrected data from the *Charles Darwin* (Fig. 5) shows that the corrected data from the two ships now agree to within 10% or better over the entire wind speed range, compared to the original differences of up to 40%. This residual difference could be accounted for by an additional 3% error in the measured wind speed, or an additional 10% displacement in the height of the flow. For the *Discovery* anemometer site, these would represent large additional airflow distortion corrections compared to the CFD results, but for the severely affected Darwin anemometer sites the additional error would be relatively small.

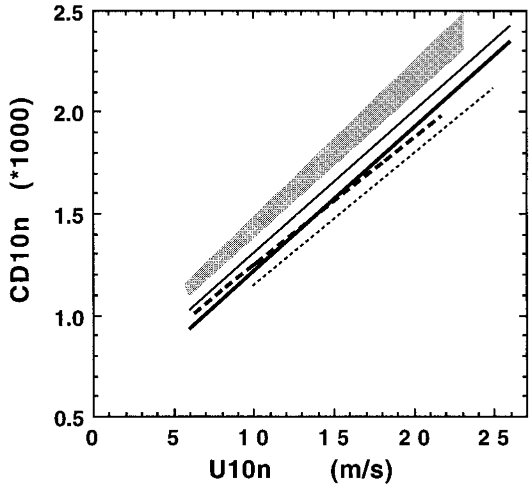

FIG. 8. The mean C_{D10n} to U_{10n} relationship from the *Discovery* data corrected for the effects of flow distortion [Eq. (3)—thick solid line]. Also shown are the open ocean relationships proposed by YT96 (thin solid line), Smith (1980) (thick dashed), and Large and Pond (1981) (dotted). The shaded region indicates the HEXOS relationship (Smith et al. 1992) for mature or fully developed seas.

b. The drag coefficient to wind speed relationship

Based on the above discussion, we have assumed that the *Darwin* data were slightly undercorrected, and have used only the much larger dataset from *Discovery* to determine the open ocean drag coefficient to wind speed relationship. This was well represented by a one-way regression of the form

$$1000C_{D10n} = 0.50 + 0.071U_{10n} \quad (6 \le U_{10n} \le 26 \text{ m s}^{-1}). \tag{3}$$

There were 1111 data points, the correlation coefficient was 0.80, and the standard errors of the intercept and slope were 0.02 and 0.002 respectively.

Figure 8 and Table 4 compare Eq. (3) with previous formulas. The new relationship gives larger C_{D10n} values than Large and Pond (1981) but, because of the CFD corrections, lower values than Yelland and Taylor (1996). The relationship confirms that suggested by Smith (1980) over most of the wind speed range.

c. The effect of airflow distortion on other open ocean C_{D10n} measurements

The airflow distortion corrections estimated by the CFD studies and the modified form of the inertial dissipation function suggested by YT96 each have the potential to significantly change the values of the derived drag coefficients. It is therefore useful to consider the possible errors that may have occurred in previous studies. Because the distribution of data with relative wind direction is not known for previous datasets, a quantified estimate of the effect of flow distortion on the observed drag coefficients cannot be made. Similarly, the lack of information with regard to the stability conditions prevents an assessment of the effect of the inertial dissipation function used. However, it is clear that these effects could combine to explain both a large percentage of the scatter in individual datasets and the mean differences between datasets. The platforms used fall into three categories: those where the airflow distortion is known to have been small, those for which the CFD modeling suggests larger correction factors, and platforms for which the airflow distortion is likely to have been large but for which quantitative estimates are not available.

Of the platforms that caused small airflow distortion, the best was undoubtedly the Bedford Institute of Oceanography (BIO) tower used by Smith (1980). This was a very stable, moored spar buoy designed to present very little obstruction to the air flow. Thus, Smith was able to use the eddy correlation method, and neither airflow corrections nor dissipation function formulation are relevant to these results. It is therefore thought that, although few in number, the 63 data obtained by Smith were least likely to suffer significant bias. In contrast to these data, all the other relationships summarized in Table 4 were obtained using the inertial dissipation technique and data from ship-mounted instruments.

TABLE 4. Drag coefficient relationships obtained in previous open ocean studies that obtained data at high wind speeds. In each case, the formulas quoted were of the form $1000C_{D10n} = a + b\,U_{10n}$ where the values of a and b quoted were those obtained by one-way regression. Also shown is the regression coefficent r, the wind speed range observed, and the number of data points. The figures in parentheses represent the standard errors of the a and b values where available.

Study	a	b	r	U_{10n} (m s^{-1})	Data	Relative wind directions (deg)
Smith (1980)	0.61	0.063	0.70	6–22	63	N/A
Large and Pond	0.49	0.065	0.74	10–26	973	−90 to +45
(1981)	1.14	0		4–10	618	
Anderson	0.49	0.071	0.91	4.5–18	84	−45 to +45
(1993)	0.59	0.065	0.83	10–18	61	
Yelland and Taylor	0.60	0.070	0.74	6–26	2298	−30 to +30
(1996)	(±0.02)	(±0.001)				
This study	0.50	0.071	0.80	6–25	1111	−10 to +10
	(±0.02)	(±0.002)				

The CFD modeling showed that the airflow distortion was relatively small for the RRS *Discovery,* the CSS *Dawson,* and, by inference, the CSS *Parizeau,* a sister ship to the *Dawson.* Our reanalysis of the YT96 data from the *Discovery* using the CFD corrections decreased the C_{D10n} values by about 6% and resulted in a C_{D10n} to U_{10n} relationship [Eq. (3)] that gives C_{D10n} values very similar to the Smith (1980) formula for most wind speeds. Anderson (1993) used data from the *Dawson* and also obtained results similar to the Smith (1980) relationship. Had he used the YT96 dissipation function, then his C_{D10n} values would have been increased by about 5%. However, for bow winds most of this increase would have been cancelled by the 3% decrease due to airflow distortion corrections and any residual bias would have been negligible considering the scatter in the data. Similar arguments apply to the Large and Pond (1982) data from a bow mast on the *Parizeau.* These data were reasonably in accord with either the Large and Pond (1981) or the Smith (1980) relationships and would be well represented by the formula proposed here [Eq. (3)].

The CFD modeling suggested that much greater airflow distortion would have affected data from the RRS *Charles Darwin* (Y94) or the CSS *Hudson* (Dobson et al. 1994, 1995). The CFD-derived corrections reduced the *Darwin* data toward the *Discovery* relationship and explained most of the difference observed between the *Hudson* and *Dawson.*

Large and Pond (1981, 1982) used data from the BIO tower and also from two ships, the weather ship *Quadra* and the F.S. *Meteor,* for which the magnitude of the airflow distortion is not known. In profile, the *Quadra* was more similar to the *Discovery* than to the *Darwin* or the *Hudson,* suggesting small airflow corrections for winds over the bow. However, the potential for significant airflow distortion existed. The foremast, where the anemometer was sited, was a very substantial structure located far aft on the foredeck, and there was a large radar dome situated over the main accommodation. Fortunately, Large and Pond were able to confirm that the *Quadra* data were comparable to the BIO tower values before merging the two datasets. Thus, for the range of relative wind directions that they used, any airflow distortion does not seem to have affected the mean C_{D10n} to U_{10n} relationship significantly. The *Meteor* (later renamed the R.V. *Rapuhia*) was in profile more similar to the *Hudson* and larger errors in the measured drag coefficient would be expected, even for winds over the bow. Studies by Augstein et al. (1974) and Rahmstorf (1988, 1989) have demonstrated the potential for large airflow distortion on this ship. Since they were well aware of this problem, Large and Pond (1982) mounted anemometers on the main mast and on a bow boom. Data were selected from each instrument according to the relative wind direction, the choice being based on comparisons with the measured wind speeds from nearby buoys. Assuming the buoy data supplied an acceptable calibration standard, the ship data would thus have been selected for minimum distortion to the airflow. In addition, the *Meteor* data were mainly obtained at wind speeds below 10 m s^{-1} and any effects of airflow distortion may have been hidden by the large scatter in the estimated C_{D10n} values.

4. The dependence of the drag coefficient on sea state

a. The expected effect of wave age on the drag coefficient

Figure 8 shows that, in the case of fully developed (C_p/U_{10n} = 1.2) or ''mature'' (C_p/U_{10n} = 1.0) seas, the Smith et al. (1992) HEXOS relationship

$$\frac{az_0}{u_*^2} = 0.48\left(\frac{C_p}{u_*}\right)^{-1} \tag{4}$$

overestimates the drag coefficient by between 15% and 25% compared to typical open ocean C_{D10n} to U_{10n} relationships. Despite this, the HEXOS formula has been applied to open ocean conditions by, for example, Gulev and Hasse (1998) who used wind and wave data from a climatology to obtain wind stress values up to 25% larger than those obtained using the formula suggested by Smith (1988). Similarly, wave-age-dependent stress formulations are sometimes incorporated into coupled ocean–atmosphere models: the wave-dependent stress relationship employed in the wind wave model of Janssen (1996, personal communication) results in open ocean C_{D10n} estimates 40% larger on average than those calculated from the *Discovery* data. However, despite the discrepancy between the HEXOS relationship and the measured mean open ocean C_{D10n} to U_{10n} relationships, it was thought that Eq. (4) might be used to explain some of the scatter in the drag coefficient measurements obtained during the *Discovery* cruises.

The *Discovery* data were collected over the open ocean, where depth and fetch did not limit the wave development. However, the wind speed varied with time and hence the sea state could be considered as duration limited (Tucker 1991). Determining the duration is not straightforward since weather systems persist over periods of days. The arrival of a front, for example, is accompanied by waves that have been influenced by the winds associated with the front for an unknown length of time. To estimate the duration, significant wave heights H_s were derived from the *Discovery's* shipborne wave recorder (SBWR) and were compared to those predicted for fully developed waves H_{sB}. This was estimated from the wind speed using the relationship suggested by Bouws (1988):

$$H_{sB} = 0.0246U_{10n}^2, \tag{5}$$

which was based on the Pierson–Moscowitz wave spectrum. The variation of the ratio H_s/H_{sB} with wind speed is shown in Fig. 9. Also shown is the ratio H_{sD}/H_{sB},

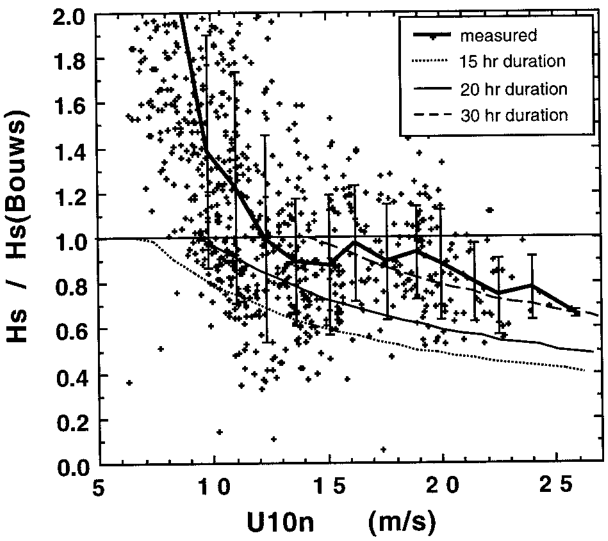

FIG. 9. Wave development with wind speed. Individual values of the ratio of the measured significant wave height from the SBWR, H_s, to that expected for a fully developed sea (from Bouws 1988) are shown (crosses), while the average values are shown by the thick solid line. The error bars indicate the standard deviation of the data. The thin lines represent the ratio predicted for different wind durations: for a fully developed sea, or infinite wind duration, the ratio would be 1.0.

where H_{sD} is the significant wave height predicted for wave development under duration-limited conditions (Tucker 1991);

$$H_{sD} = 0.0146D^{5/7}U^{9/7}, \tag{6}$$

and D is the duration in hours.

In the mean, for wind speeds of 12 m s^{-1} or less, the waves were fully developed: values of the ratio greater than one indicate the presence of swell. Above 15 m s^{-1}, the mean value of H_s/H_{sB} indicates that the measured wave heights correspond to those expected for a wind speed duration of 30 hours. Individual data suggest duration times of 15 hours or less. It must be emphasized that the SBWR will overestimate H_s when swell is present, that is, at all wind speeds, the duration of the wave development will generally be less than that suggested by the SBWR data.

In order to estimate the range of variation in the drag coefficient estimates that could be expected from the duration-limited wave development, the frequency, f_p, of the peak of the wave spectrum was calculated from (Tucker 1991):

$$f_p^{-1} = 0.540D^{3/7}U^{4/7}. \tag{7}$$

Durations of 15 upward hours were assumed. The resulting C_p/u_* estimates were then used in the HEXOS formula (4). This suggested that C_{D10n} anomalies of the order of 10% should be seen. Larger anomalies would occur if, as thought, the duration has been overestimated due to the presence of swell increasing the estimate of H_s. Of most importance, the C_{D10n} anomalies caused by the duration-limited wave development should, by definition, persist for periods of at least a few hours.

b. The effects of wave age on the observed drag coefficient

The friction velocity estimates obtained during the *Discovery* cruises were scattered about a mean u_* to U_{10n} relationship with a standard deviation of almost 9%: equivalently, the scatter of the drag coefficients about the mean relationship was 18%. This is consistent with the rms errors of 3% for wind speed and 6% for u_* estimated from instrument comparisons on the RRS *Darwin* by Yelland et al. (1994). This suggests that the scatter in the *Discovery* data could be completely accounted for by random experimental errors. However, the results from the *Discovery* cruises were examined for systematic deviations from the mean C_{D10n} to U_{10n} relationship, which could be attributed to changes in the sea state. To this end, the percentage C_{D10n} ''anomalies,'' ΔC_D, were calculated from

$$\Delta C_D = 100\frac{(C_{D10N} - C_{DFIT})}{C_{DFIT}}, \tag{8}$$

where C_{DFIT} was calculated from the measured U_{10n} using the relationship (3).

Yelland (1997) examined the *Discovery* data for evidence of sea-state-dependent C_{D10n} anomalies; no statistical links with either wave age, duration of wave development, or wind history were found. Persistent anomalies could only be seen if the data were smoothed, using a running 2-h ''top hat'' filter, which reduced the standard deviation of the ΔC_D estimates from 18% to 7%. Some small anomalies were seen to persist for an hour or so in the smoothed data, but could not be associated with either sea state or wind history.

One exceptionally large and persistent anomaly occurred during a storm where the wind speed reached a maximum of more than 23 m s^{-1} during the night of 13 January 1993. The time series of smoothed data obtained during this storm are shown in Fig. 10. The logging system for the anemometer failed at the peak of the storm and was not restarted until 6 hours later. It can be seen that, as the wind speed increased from 18 to over 23 m s^{-1}, the ΔC_D estimates were very small, whereas during the 12 hours over which the wind decreased to 15 m s^{-1}, the ΔC_D estimates averaged between 5% and 10%. While the wind speed was increasing, the true wind direction was fairly steady at 275°, but had shifted by about 20° by the time the logging system had resumed working. However, it can clearly be seen that the enhancement of the C_{D10n} estimates correlates much more closely with the change in the relative wind direction than with the changes in the wind speed or true wind direction. It is therefore evident that the apparent C_{D10n} ''anomaly'' was due to the changing effects of flow distortion and was

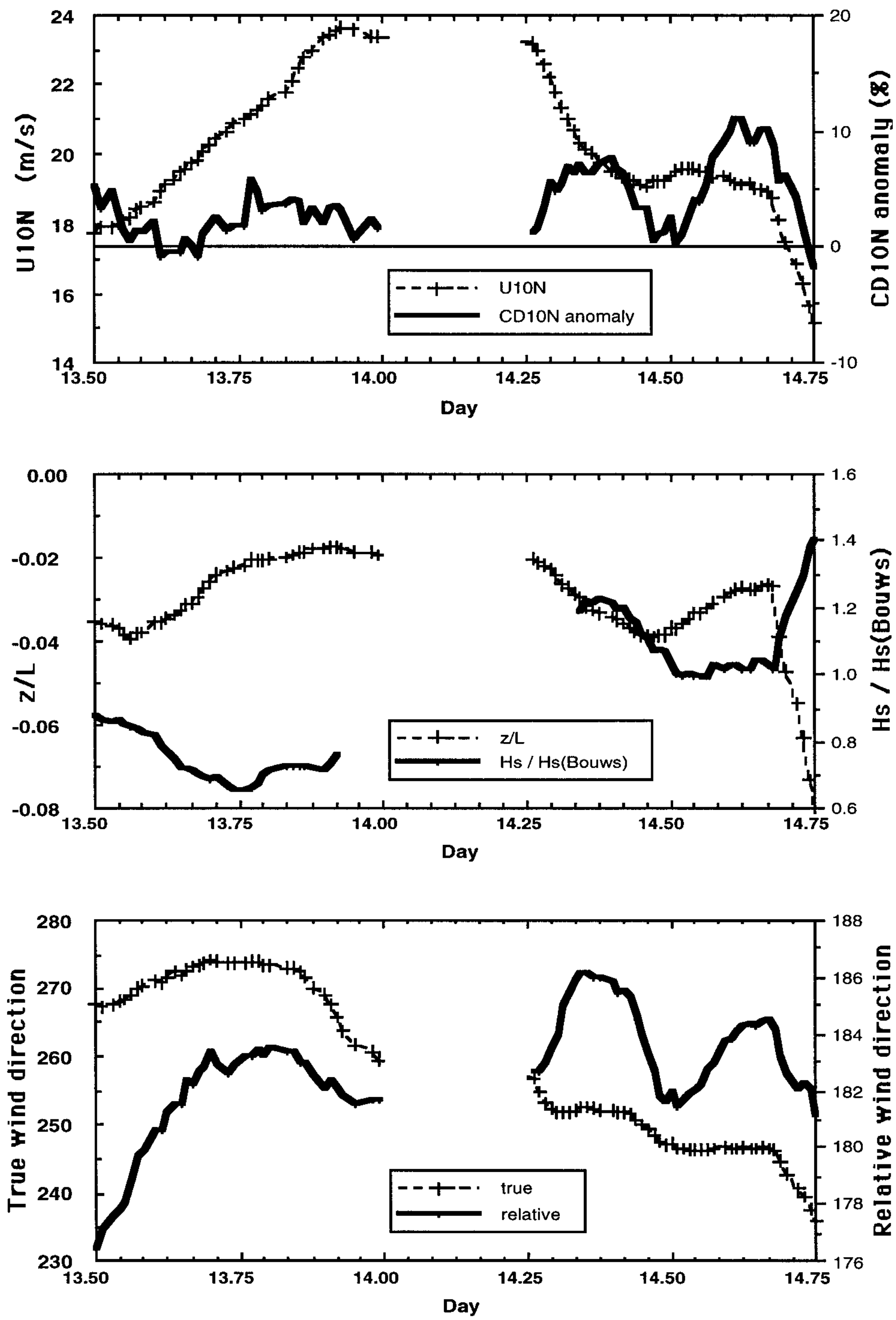

FIG. 10. Time series of data smoothed with a running 2-h filter; (top) U_{10n} and $\triangle C_D$, (middle) stability parameter and wave development, and (bottom) true and relative wind directions. The data shown begins at 1200 LT 13 January and ends at 1800 LT 14 January.

not due to any change in the sea state. Very careful observations would be essential in any study aimed to unambiguously associate drag coefficient anomalies with changes in the wave field.

It is concluded that wave-age-dependent parameterizations of the wind stress, such as that suggested from the HEXOS experiment, are redundant for open ocean conditions.

c. Implications for previous studies

It has been shown that the effects of airflow distortion can vary rapidly with a change in relative wind direction (Figs. 1b, 2, and 10). This relative wind direction dependence must be taken into consideration when examining anomalies in the observed drag coefficient. For example, Anderson (1993), Large and Pond (1981, 1982), and Yelland and Taylor (1996) all used data obtained over rather wide ranges of relative wind direction (Table 4). The wind tunnel results and the CFD modeling both suggest that airflow distortion would be capable of causing variations of C_{D10n} similar in magnitude to the reported scatter in the observations. In addition, research ships when on station or hove-to tend to be oriented with respect not only to the wind but also to any significant wind sea or swell. A change in the swell conditions may cause the ship's orientation to be altered, thus changing the relative wind direction. The resulting change in airflow distortion could cause a spurious change in the observed C_{D10n} values, which would then appear to be associated with the change in sea conditions.

The lack of observed drag coefficient anomalies in the *Discovery* data contrasts with the large anomalies found over the open ocean in previous studies, as described by Large and Pond (1981) and by Denman and Miyake (1973). In both these studies, coherent anomalies of the order of 20% of the mean drag coefficient were seen to persist for periods of a few hours and were attributed to changes in the sea state. Denman and Miyake used a shipborne anemometer to obtain the wind speed and stress measurements, and data were accepted from a range of relative wind directions spanning 180°. Estimates of the flow distortion were not available and no corrections were made for non-neutral atmospheric stability. The results were so scattered that the authors concluded that the drag coefficient did not depend on the wind speed, which ranged from 4 to 17 m s^{-1}, or on atmospheric stability. The observed dependence of the drag coefficient on the sea state could have been due to either the assumption of a constant drag coefficient, to a change in the flow distortion with relative wind direction, to the lack of stability corrections, or any combination of these. In contrast, the results from the Large and Pond experiment were both more numerous and of higher quality. These authors also reported an increase in the dissipation-derived drag coefficient estimates after the passage of a storm. The data in question were obtained from an anemometer mounted on the Bedford Institute of Oceanography tower, so, although there was a large coincident shift in the wind direction, the effects of flow distortion may not have been significant. However, the anomaly was observed during wind speeds of around 5 m s^{-1} and for rather stable conditions ($z/L \geq 0.2$): the accuracy of the dissipation method under such conditions is rather doubtful (Yelland 1997). Indeed, over the wind speed range of 4–10 m s^{-1}, the results of Large and Pond were so scattered that they showed no variation with wind speed and were represented by a constant C_{D10n} value. More recent studies (Yelland and Taylor 1996; Dupuis et al. 1997) have shown that the C_{D10n} to U_{10n} relationship has a minimum at about 6 m s^{-1} and that an increase in C_{D10n} with decreasing wind speeds is to be expected.

d. Discussion

The present study shows that the wind stress over the open ocean can be well represented by a simple C_{D10n} to U_{10n} relationship and that the effects of sea state on this relationship are insignificant. The scatter in the *Discovery* drag coefficient estimates could not be related to the sea state, but could be explained entirely by experimental noise. The open ocean sea-state effects described by previous authors are thought to have been due to the effects of flow distortion or to other experimental causes. The effects of flow distortion seem to be of particular importance since the impact on the drag coefficient estimate is both large and very sensitive to changes in the relative wind direction

The lack of any significant effect of the sea state on the open ocean wind stress could be due either to 1) an absence of young waves due to the persistence of weather systems or 2) the presence of swell. The mechanism by which the presence of swell could suppress the characteristics of young wind seas is not known. However, no reliable evidence for a wave age dependence of the wind stress has been reported for cases where swell waves are present. For example, Dobson et al. (1994) were unable to verify the HEXOS formula in open ocean conditions. Indeed, Smith et al. (1996), in their review of the HEXOS program, state that the application of the HEXOS formula should be restricted to sites with a water depth of 18 m or to wind speeds below 13 m s^{-1}. However, the results from the present study suggest that the formula is not applicable in the open ocean even at the lower wind speeds. Again, this may be due to the prevalence of swell in the open ocean: Smith et al. (1996) state that the dependence of the wind stress on the wave age was only apparent for single-peaked wave spectra.

In addition to the lack of evidence for a wave age dependency of the open ocean wind stress, the validity of wave age relationships derived from coastal and lake experiments is also now being questioned (e.g., Janssen 1997). For example, Oost (1997) reexamined the HEXOS data and found that the reported wave age dependence of the wind stress (Smith et al. 1992) was more likely to have been caused by the long wavelength waves shoaling and steepening into shallowing water, rather than by the presence of underdeveloped waves. Anctil and Donelan (1996) described a similar effect of the wave steepness on the wind stress measured over Lake Ontario.

5. Summary and conclusions

This study examined open ocean drag coefficient measurements for evidence of significant anomalies that can be related to sea state or wave age. None were found. It is thought that such anomalies, which have been described by previous authors, were caused by experimental errors rather than changes in the sea state. It has been shown that the effects of flow distortion can produce such spurious anomalies.

The presence of the ship, or other large instrument platform, will cause systematic errors in the measurement of the drag coefficient, even if the anemometer is sited in a carefully chosen, well-exposed position. The effects of flow distortion are twofold: the flow can be both displaced vertically and either accelerated or decelerated. If the inertial dissipation method is used these effects cause biases in the calculation of the friction velocity and the true wind speed respectively. However, if the magnitude of the flow distortion effects can be quantified (for a particular relative wind direction), then the necessary corrections are straightforward. In contrast, if the eddy correlation technique is employed then correcting for the effects of flow distortion is rather more complicated (Oost et al. 1994).

Use of a three-dimensional CFD model successfully reproduced the wind speed errors at anemometer sites on two Canadian research ships that had previously been determined using wind tunnel studies (Surry et al. 1989; Thiebaux 1990). The CFD model was also used to simulate the flow of air around the RRS *Charles Darwin*: the results of this simulation reconciled the previously disparate drag coefficient results from four anemometers mounted on the foremast of the ship. After this initial validation, the CFD software was used to quantify the effects of flow distortion at an anemometer site on the RRS *Discovery*. This showed that, although the anemometer was well sited on a relatively streamlined platform, the initial estimates of the drag coefficient were overestimated by about 6%. The corrected drag coefficient data, selected for a narrow range of relative wind directions ($\pm 10°$ of the ship's bow), confirmed the earlier open ocean relationship suggested by Smith (1980) from a more limited set of data.

The wind tunnel studies and the extensive *Discovery* dataset both showed that the effects of flow distortion are sensitive to changes in the relative wind direction. For example, the mean C_{D10n} to U_{10n} relationship changed by about 10% when the relative wind direction changed from bow-on to 20° to port of the bow of the *Discovery*. This implies that much of the scatter found in any drag coefficient dataset could be caused by the effects of flow distortion varying with changes in the wind direction. Much care is needed when examining such a dataset. Apparent anomalies in the drag coefficient might be erroneously ascribed to a change in the sea state or to a change in the angle between the wind and the waves, whereas this rather more mundane problem may be the true cause.

It is believed that the scatter in the open ocean drag coefficient estimates is caused by experimental factors. The lack of any significant sea-state dependence of the wind stress over the open ocean contrasts with the enhanced drag coefficients observed by other researchers over coastal waters and lakes. It is not known whether this disagreement is due to an absence of "young" waves in the open ocean or to the enhanced coastal stresses being caused by shoaling, rather than young, waves. However, it is clear that the use of a wave-age-dependent parameterization of the wind stress is redundant for open ocean conditions.

Acknowledgments. We are grateful to Dr. M. Smith, of the University of Manchester Institute of Science and Technology, for providing the Kaijo-Denki and Bivane data from the *Charles Darwin*, and to colleagues at the Bedford Institute of Oceanography, Nova Scotia, for providing ship plans and helpful discussion. We appreciate the support given by the staff of Ricardo Consulting Engineers Ltd. (Shoreham-by-Sea, U.K.), especially that of Karl John, and of FEMSYS Ltd. (Leicester, U.K.). The research was partly funded by the Atmospheric Environment Service of Canada.

REFERENCES

Anctil, F., and M. A. Donelan, 1996: Air–water momentum flux observations over shoaling waves. *J. Phys. Oceanogr.,* **26,** 1344–1353.

Anderson, R. J., 1993: A study of wind stress and heat flux over the open ocean by the inertial dissipation method. *J. Phys. Oceanogr.,* **23,** 2153–2161.

Augstein, E., H. Hoeber, and L. Kruegermeyer, 1974: Fehler bei temperatur-, feuchte- und windmessungen auf schiffen in tropischen Breiten. *"Meteor" Forschungsergeb.,* **B9,** 1–10.

Blanc, T. V., 1986: Superstructure flow distortion corrections for wind speed and direction measurements made from Tarawa Class (LHA1-LHA5) ships. NRL Rep. 9005, 20 pp. [Available from Naval Research Laboratory, Washington, DC 20375-5000.]

——, 1987: Superstructure flow distortion corrections for wind speed and direction measurements made from Virginia Class (CGN38-CGN41) ships. NRL Rep. 9026, 24 pp. [Available from Naval Research Laboratory, Washington, DC 20375-5000.]

Bouws, E., 1988: Basic definitions and descriptions of ocean waves. *Guide to Wave Analysis and Forecasting,* World Meteorological Organization Publ. 702, 23–25.

Charnock, H., 1955: Wind stress on a water surface. *Quart. J. Roy. Meteor. Soc.,* **81,** 639–640.

Ching, J. K. S., 1976: Ship's influence on wind measurements determined from BOMEX mast and boom data. *J. Appl. Meteor.,* **15,** 102–106.

Denman, K. L., and M. Miyake, 1973: Behaviour of the mean wind, the drag coefficient, and the wave field in the open ocean. *J. Geophys. Res.,* **78,** 1917–1931.

Dobson, F. W., S. D. Smith, and R. J. Anderson, 1994: Measuring the relationship between wind stress and sea state in the open ocean in the presence of swell. *Atmos.–Ocean,* **32,** 237–256.

——, ——, and ——, 1995: Open-ocean measurements of the wind stress–sea state relationship. *Proc. Fourth Int. Workshop on Wave Hindcasting and Forecasting,* Banff, AB, Canada, Environment Canada, 171–176.

Donelan, M. A., 1990: Air–sea interaction. *The Sea*, B. Le Mehaute and D. M. Hanes, Eds., Wiley-Interscience, 239–292.

——, F. Dobson, S. D. Smith, and R. A. Anderson, 1993: On the dependence of sea surface roughness on wave development. *J. Phys. Oceanogr.,* **23,** 2143–2149

Dupuis, H., P. K. Taylor, A. Weill, and K. Katsaros, 1997: The inertial dissipation method applied to derive turbulent fluxes over the ocean during the SOFIA/ASTEX and SEMAPHORE experiments in low to moderate wind speeds. *J. Geophys. Res.,* **102** (C9), 21 115–21 129.

Edson, J. B., C. W. Fairall, P. G. Mestayer, and S. E. Larsen, 1991: A study of the inertial-dissipation method for computing air–sea fluxes. *J. Geophys. Res.,* **96** (C6), 10 689–10 711.

Femsys, 1994: FEMGEN/FEMVIEW user's manual. Femsys Ltd., Leicester, United Kingdom, 523 pp. [Available from Femsys Ltd., 158 Upper New Walk, Leicester LE1 7QA, United Kingdom.]

Geernaert, G., 1990: The theory and modelling of wind stress with applications to air–sea interaction and remote sensing. *Rev. Aquatic Sci.,* **2,** 125–149.

Godshall, F. A., W. R. Seguin, and P. Sabol, 1976: Analysis of ship surface meteorological data obtained during GATE intercomparison periods. NOAA Tech. Rep. EDS 17, 73 pp. [Available from National Technical Information Service, U.S. Dept. of Commerce, Springfield, VA 22161.]

Gulev, S. K., and L. Hasse, 1998: North Atlantic wind waves and wind stress fields from voluntary observing ship data. *J. Phys. Oceanogr.,* **28,** 1107–1130.

Henjes, K., 1996: Isotropic and anisotropic correlations in turbulent wind speed data. *Bound.-Layer Meteor.,* **84,** 149–167.

Janssen, J. A. M., 1997: Does wind stress depend on sea-state or not? A statistical error analysis of HEXMAX data. *Bound.-Layer Meteor.,* **83,** 479–503.

Kahma, K. K., and M. Lepparanta, 1981: On errors in wind speed observations on R/V Aranda. *Geophysica,* **17,** 155–165.

Kidwell, K. B., and W. R. Seguin, 1978: Comparison of mast and boom wind speed and direction measurements on US GATE B-scale ships. NOAA Tech. Rep. EDS 28, 41 pp. [Available from National Technical Information Service, U.S. Dept. of Commerce, Springfield, VA 22161.]

Large, W. G., and S. Pond, 1981: Open ocean momentum flux measurements in moderate to strong winds. *J. Phys. Oceanogr.,* **11,** 324–336.

——, and ——, 1982: Sensible and latent heat flux measurements over the ocean. *J. Phys. Oceanogr.,* **12,** 464–482.

Nordeng, T. E., 1991: On the wave age dependent drag coefficient and roughness length at sea. *J. Geophys. Res.,* **96,** 7167–7174.

Oost, W. A., 1997: The KNMI HEXMAX stress data—A revisit. *Bound.-Layer Meteor.,* in press.

——, C. W. Fairall, J. B. Edson, S. D. Smith, R. J. Anderson, J. A. B. Wills, K. B. Katsaros, and J. DeCosmo, 1994: Flow distortion calculations and their application in HEXMAX. *J. Atmos. Oceanic Technol.,* **11,** 366–386.

Queffeulou, P., 1991: Accuracy of wind measurements performed on buoys, ship, and island during the TOSCANE-2 Experiment. *J. Atmos. Oceanic Technol.,* **8,** 835–855.

Rahmstorf, S., 1988: Wind observations from RV Rapuhia. DSIR Internal Rep. 88/2, 12 pp. [Available from Division of Marine and Freshwater Science, DSIR, Wellington, New Zealand.]

——, 1989: Improving the accuracy of wind observations from ships. *Deep-Sea Res.,* **36,** 1267–1276.

Reynolds, R. M., 1982: Comparison of surface meteorological observations from ship and toroid buoy in the North Pacific during STREX. *J. Appl. Meteor.,* **21,** 1032–1037.

Ricardo, 1994: VECTIS Computational Fluid Dynamics user's guide. Ricardo Consulting Engineers Ltd., Shoreham-by-Sea, United Kingdom, 112 pp. [Available from Ricardo Consulting Engineers Ltd., Bridge Works, Shoreham-by-Sea, West Sussex BN43 5FG, United Kingdom.]

Romanov, Y. A., I. B. Fedorova, M. S. Chervyakov, and G. I. Shapiro, 1983: An improvement in the accuracy of shipboard measurements of wind speed and direction based on aerodynamic tests of a ship model. *Oceanology,* **23,** 267–270.

Smith, S. D., 1980: Wind stress and heat flux over the ocean in gale force winds. *J. Phys. Oceanogr.,* **10,** 709–726.

——, 1988: Coefficients for sea surface wind stress, heat flux and wind profiles as a function of wind speed and temperature. *J. Geophys. Res.,* **93,** 15 467–15 474.

——, and Coauthors, 1992: Sea surface wind stress and drag coefficients: The HEXOS results. *Bound.-Layer Meteor.,* **60,** 109–142.

——, K. B. Katsaros, W. B. Oost, and P. G. Mestayer, 1996: The impact of the HEXOS programme. *Bound.-Layer Meteor.,* **78,** 121–141.

Surry, D., R. T. Edey, and I. S. Murley, 1989: Speed and direction correction factors for shipborne anemometers. Engineering Science Research Rep. BLWT-SS9-89, University of Western Ontario, London, ON, Canada, 83 pp. [Available from University of Western Ontario, London, ON N6A 5B9, Canada.]

Thiebaux, M. L., 1990: Wind tunnel experiments to determine correction functions for shipborne anemometers. Canadian Contractor Report of Hydrography and Ocean Sciences 36, Bedford Institute of Oceanography, Dartmouth, NS, Canada, 57 pp. [Available from Bedford Institute of Oceanography, Dartmouth, NS B2Y 4A2, Canada.]

Tillman, J. E., L. Landberg, and S. E. Larsen, 1994: The boundary layer of Mars: Fluxes, stability, turbulent spectra, and growth of the mixed layer. *J. Atmos. Sci.,* **51,** 1709–1727.

Tucker, M. J., 1991: *Waves in Ocean Engineering.* Ellis Horwood, 431 pp.

Weller, R. A., R. E. Payne, W. G. Large, and W. Zenk, 1983: Wind measurements from an array of oceanographic moorings and from F/S Meteor during JASIN 1978. *J. Geophys. Res.,* **88**(C14), 9689–9705.

——, D. L. Rudnick, R. E. Payne, J. P. Dean, N. J. Pennington, and R. P. Trask, 1990: Measuring near-surface meteorology over the ocean from an array of surface moorings in the subtropical convergence zone. *J. Atmos. Oceanic Technol.,* **7,** 85–103.

Wu, J., 1980: Wind stress coefficients over the sea surface near neutral conditions—A revisit. *J. Phys. Oceanogr.,* **10,** 727–740.

Yelland, M. J., 1997: Wind stress over the open ocean. Ph.D. thesis, University of Southampton, Southampton, United Kingdom, 168 pp.

——, and P. K. Taylor, 1996: Wind stress measurements from the open ocean. *J. Phys. Oceanogr.,* **26,** 541–558.

——, ——, K. G. Birch, R. W. Pascal, and A. L. Williams, 1991: Evaluation of a solent sonic anemometer on RRS Charles Darwin Cruise 43. Institute of Oceanographic Sciences, Rep. 288, 55 pp. [Available from Southampton Oceanography Centre, Southampton SO14 3ZH, United Kingdom.]

——, ——, I. E. Consterdine, and M. H. Smith, 1994: The use of the inertial dissipation technique for shipboard wind stress determination. *J. Atmos. Oceanic Technol.,* **11,** 1093–1108.